

Timing quantum emission: coherence, superradiance, and entanglement in order

Nur Fadhillah Binti Rahimi,¹ Norman Koo Tze Wei,² Daniel Schumayer,^{1,3}
Christopher Gies,⁴ Leong Chuan Kwek,^{2,5,6,7} and David A. W. Hutchinson^{1,2}

¹*Dodd-Walls Centre for Photonic and Quantum Technologies,
Department of Physics, University of Otago, New Zealand*

²*Centre for Quantum Technologies, National University of Singapore, Singapore*

³*School of Physics, University of Sydney, Australia*

⁴*Institute of Physics, Carl von Ossietzky University of Oldenburg, Germany*

⁵*Institute of Advanced Studies, Nanyang Technological University, Singapore*

⁶*National Institute of Education, Singapore*

⁷*MajuLab, CNRS-UNS-NUS-NTU International Joint Research Unit, Singapore*

(Dated: December 9, 2025)

We investigate the short-term temporal dynamics of superradiance in closely spaced quantum emitters. Building on Dicke's 1954 framework, we analyze the sequential emergence of coherence, superradiance, and entanglement, revealing a distinct temporal hierarchy in their extremal values: relative coherence develops first, followed by the peak of correlated emission, then minimal entanglement, and finally correlated dephasing. These findings suggest that enhanced relative coherence initiates correlated emission, and when correlated dephasing is negligible, entanglement and correlated emission become tightly linked in time.

Introduction — In 1954 Robert Dicke proposed a novel description of spontaneous light emission in a system of particles coupled to an electromagnetic field [1]. Prior, the concept of light emission had been described as radiation of photons emitted by *independent* particles, which is indeed justified if the typical distance between randomly distributed particles is larger than the wavelength of emitted light waves. However, if the close proximity of particles cannot be neglected, spontaneous light emission is better described as a *collective*, self-organization phenomenon [2]: particles become correlated due to each other's radiation field.

A system of two-level emitters, archetypically represented by spin- $\frac{1}{2}$ particles, that are prepared in their individual excited states eventually decays to the ground state by emitting photons spontaneously. For indepen-

dent emitters the decay rate is proportional to the number of emitters, N [1], while for correlated emitters it scales as N^2 , which is a well-established signature of superradiant emission [3]. Consequently, the peak photon emission rate appears as a sudden burst of radiation, hence the term 'superradiance,' that fundamentally relies on the correlations among emitters.

Superradiance and superfluorescence [4], can be highly beneficial for quantum-enhanced measurements and quantum metrology [5]: a steady-state superradiant lasing with its ultra-narrow line-width [6, 7] would improve optical clock frequencies [8] and spectroscopically relevant transitions [8–10], or allow for terahertz amplifiers [11], optical emitters [12]. Furthermore, the critical behavior near superradiant phase transitions permits reaching Heisenberg-limit in measurements [13].

Superradiance is not only useful because the peak intensity scales with N^2 , but also due to its tunability. It was first demonstrated in thermal gases [14, 15], and later in single diamond nanocrystals [16], while superfluorescence was observed in spatially inhomogeneous systems, in colloidal perovskite nanocrystals [17, 18]. Recently superfluorescent emitters were coupled to nanoparticles at *room temperature* [19]; an immense step away from cryogenic experimental setups towards applications. An intense laser pulse (ns or fs) excites many lanthanide ions within a single nanoparticle forming a collective quantum state that emits light faster than usual: emission lifetime shortens from μ s down to ns. In semiconductor systems, a recombination-time shortening by a factor of 40, down to 20 ps has been reported [20].

Nowadays, it is instructive to understand how and when a system reaches the superradiant state, and to quantify how superradiance, coherence, and entanglement relate during evolution. Earlier, we established [21]

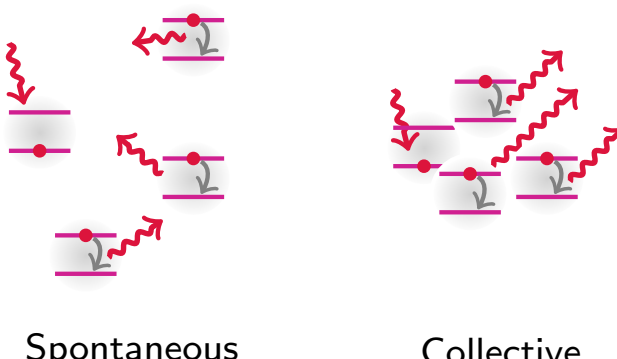


FIG. 1. (Color online) Schematics of spontaneous radiation and superradiant emission. On the left, emitters are far apart and decay individually following a characteristic rate, while on the right the emitters are influenced by each other's radiation field, hence are constructively coupled.

a close connection between emitter correlations and an entanglement witness sensitive to Dicke-states. From a quantum resource-theory perspective, it also seemed natural to ask: what drives superradiance? Does coherence build up and then get converted into superradiance, or is entanglement, as the resource, converted into coherence or superradiance? Such questions are far from trivial, e.g., Bassler has just proven [22] that a system initially prepared in a fully inverted Dicke state, while undergoing superradiance, does not generate entanglement. Rosario *et al.* reached a similar conclusion using entanglement of formation [23]. Ferioli *et al.* [24] explored that coherence varies during superradiant emission: both first and second-order coherence emerge during the initial development of superradiance peak, but subsequently drop and indicate anticorrelations (photons are unlikely to be emitted simultaneously) after which it settles to a stable value (subradiant phase). Furthermore, local observables can be well-approximated via a mean-field approach, even if a considerable amount of entanglement is generated in super- and subradiant decay processes [25]. In this Letter, we investigate the temporal characteristics: in what sequence coherence, entanglement and superradiance build up.

Formalism — The original Dicke-model qualitatively explains superradiance, but it is insufficient to describe realistic systems, as it considers only the decay of emitters. In practice, the emitters' dynamics and interaction with the electromagnetic field are intertwined. The model also assumes that emitters are much closer than the emitted photon's wavelength which requires the inclusion of dipole-dipole interactions. If this interaction, combined with collective decay, is sufficiently strong, it may break the global symmetry (conservation of parity of the total number of excitations), and may lead to a phase transition from the normal to the superradiant state [26–30].

The Tavis-Cummings hamiltonian [28, 31] governs N identical two-level emitters coupled to photons

$$H = \frac{1}{2}\omega_q \sum_{i=1}^N \sigma_i^z + g \sum_{i=1}^N (\sigma_i^+ \alpha + \sigma_i^- \alpha^\dagger) + \omega_c \alpha^\dagger \alpha, \quad (1)$$

where ω_q is the resonance frequency of an emitter, g is the coupling strength of an emitter and a photon, while ω_c is the angular frequency of a photon.

In an open quantum system, incoherent processes, such as decay, photon loss and pure dephasing at rates γ , κ and γ_ϕ , can be captured within a Markovian approximation and Lindblad master equation

$$\frac{d}{dt}\rho = -i[H, \rho] + \sum_{k \in \{\gamma, \kappa, \gamma_\phi\}} D_k(\rho), \quad (2)$$

where D_k follows the standard Lindbladian structure

$$D_k(\rho) = k \left[L_k \rho L_k^\dagger - \frac{1}{2} \{ L_k^\dagger L_k, \rho \} \right]$$

with $L_\gamma = \sigma^- \otimes \mathbf{I}$, $L_\kappa = \mathbf{I} \otimes \alpha$, and $L_{\gamma_\phi} = \sigma^z \otimes \mathbf{I}$.

Here we solve Eq. (2) using two approaches. Exact calculation for $N < 10$ is feasible and suits experimental setups based on superconducting qubits, quantum dots [32, 33], or the silicon-on-insulator platform [34]. If, however, emitters are indistinguishable and permutation invariance holds, the calculation extends to $N \leq 60$ using an optimised numerical approach [35]. We consider the situation in which all emitters occupy the de-excited ground states, while $\frac{1}{2}N$ photons populate the a resonant mode of the quantized electromagnetic field [36, 37].

We investigate the temporal evolution of four quantities: correlated emission, $C_0 = \langle \sigma_i^+ \sigma_j^- \rangle$, the von Neumann entropy, $S(\rho) = -\text{Tr}(\rho \ln \rho)$, the relative entropy of coherence [38], $C_{\text{rel}} = S(\rho_{\text{diag}}) - S(\rho)$, and the entanglement witness, $\langle W \rangle = 1 - 4\text{Re}(C_0) + C_{zz}$ [39]. Note that C_0 is related to W via correlated dephasing, $C_{zz} = \langle \sigma_i^z \sigma_j^z \rangle$ ($i \neq j$). We note that C_0 and S are basis-independent, while $\langle W \rangle$ and C_{rel} are not.

Timescales during superradiant emission — In order to quantify the temporal evolution we introduce characteristic times for each of these quantities which measures when they reach their extremal value. Within the independent, single-particle picture the emitters decay at a linear rate, hence the characteristic timescale is $\tau \propto \frac{1}{N}$ [40]. If, however, phase dispersion is approximately zero and particles exhibit collective behavior, the

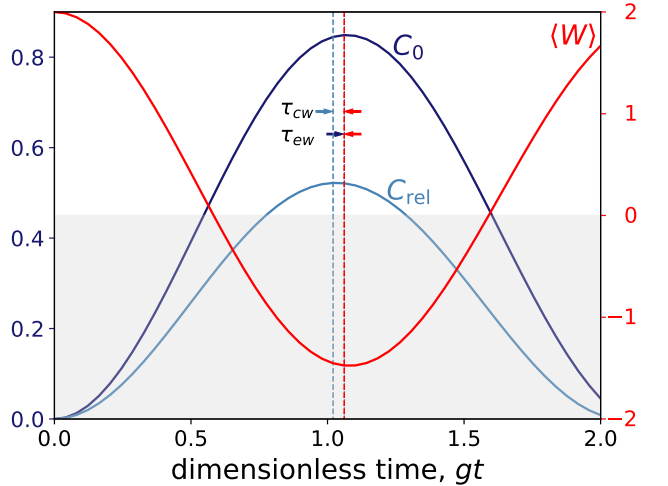


FIG. 2. (Color online) Correlated emission, relative entropy of coherence, and entanglement witness are shown for the $N = 2$ emitter subsystem as functions of dimensionless time. Correlated emission and relative entropy of coherence are measured on the left ordinate, while entanglement witness is measured on the right ordinate (see colors). Vertical lines indicate those moments in time, where each quantity reaches its extremal value. In this setup C_{rel} , reaches its maximum first, then C_0 and $\langle W \rangle$ reach their extrema simultaneously. The corresponding time differences are τ_{cw} (coherence vs. witness) and τ_{ew} (emission vs. witness). Other parameters: $g = 1$, $\gamma/g = 0.1$, $\kappa/g = 0.1$, and $\gamma_\phi/g = 0.0225$.

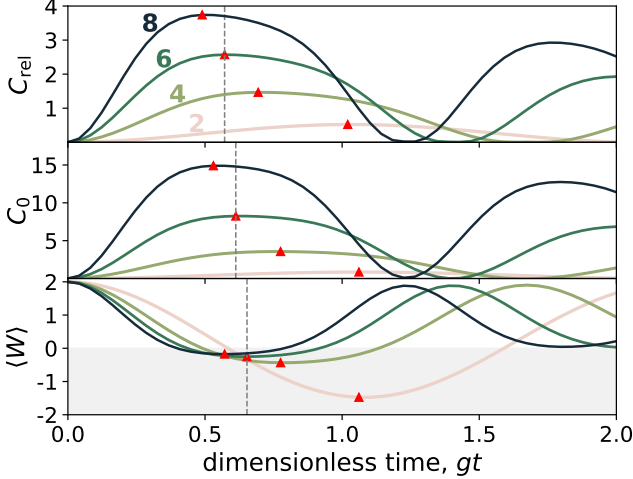


FIG. 3. (Color online) Time evolution of C_{rel} , C_0 , and $\langle W \rangle$, are plotted for $N = 2, 4, 6$, and 8 emitters. The number of emitters are shown in the top figure as labels and different colors. The colors are common in all subplots. Vertical dashed lines indicate the moments when these quantities reach their extrema for $N = 6$. Other parameters are as in Fig. 2.

system reaches phase synchronization culminating in superradiant emission, which is associated with a characteristic time [41, 42]

$$\tau_{C_0} \approx \tau \ln(N) \approx \frac{\ln(N)}{N}.$$

Since $\tau_{C_0} \propto N^{-1}$, the larger the system the sooner it becomes superradiant. Extremal phase dispersion and maximum radiation intensity occur simultaneously, reinforcing that phase synchronization is the mechanism that gives rise to superradiance. This behavior may be advantageous for quantum metrology purposes [42, 43].

Figure 3(a) shows the evolution of relative coherence, correlated emission, and the expectation value of the entanglement witness for small systems ($N = 2, 4, 6, 8$). All measures reach their extremal values, denoted by small red triangles, earlier as system size increases—a well-known result for C_0 . Additionally, for fixed N the coherence, C_{rel} builds up first, followed by correlated emission, C_0 , and finally entanglement. These moments when each of these quantities peak are marked by vertical dashed lines for $N = 6$. Based on this observation we conjecture that

$$\tau_{C_{\text{rel}}} \leq \tau_{C_0} \leq \tau_W.$$

Equality can happen, e.g., for $N = 2$, $\tau_{C_{\text{rel}}} < \tau_{C_0} = \tau_W$. Note that the inequality $\tau_{C_{\text{rel}}} < \tau_W$ suggests a potential causal relationship between C_{rel} and entanglement. This finding supports a prior mathematical study [44]: coherence can be converted into entanglement. Yet, further microscopic analysis is needed to uncover the process of such conversion. Fig. 4 depicts the expected qualitative

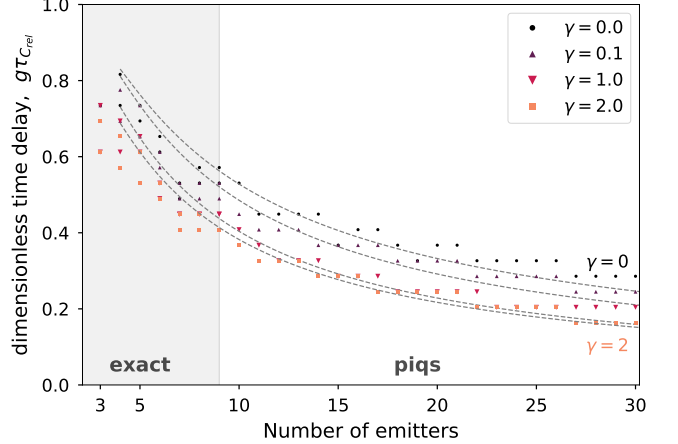


FIG. 4. (Color online) Time-delay, $\tau_{C_{\text{rel}}}$ is depicted as a function of N . The shaded area, $N \leq 9$, is calculated using two different approaches: exact time-evolution in computational basis and a permutational invariant quantum solver (PIQS). These approaches lead to similar values. The four sets of data, distinguished by different markers and colors, correspond to different decay parameters, $\gamma = 0, 0.1, 1, 2$. Qualitatively, $\tau_{C_{\text{rel}}}$ diminishes as $\ln(N)/N^\alpha$, where $\alpha \approx 1$ for $\gamma = 0$, and $\alpha \approx 1.2$ for $\gamma = 2$, as shown by the dashed lines. Similar results apply to τ_{C_0} and τ_W , but left out for clarity.

behavior of dimensionless time delay $g\tau_{C_{\text{rel}}}$ as a function of N and γ ; with increasing N the time delay decreases as $\ln(N)/N^\alpha$, where α is a fitted parameter assumed to be weakly dependent on γ . Indeed for no emitter decay we recover the classical result $\alpha = 1$, however, with increasing dissipative process the reduction of time delay is slightly more pronounced, $\alpha \approx 1.2$ for strong decay. The case is qualitatively similar to that of a damped harmonic oscillator, whose first extremal deflection shifts to earlier times $\tau_1 \propto (\omega_0^2 - \beta^2)^{-1/2}$ with increasing mechanical damping β . Here, ω_0 is the angular frequency of the undamped harmonic oscillator.

Finally, in Fig. 5 the behavior of time differences between three measures are studied as a function of the light-matter coupling strength, keeping C_{rel} as the baseline. We find that that τ_W is always larger than τ_{C_0} , and also that any kind of time difference vanishes as the coupling strength increases. This latter effect is expected, since for increasing g the system exhibits faster Rabi oscillations between collective atomic states and the cavity mode, and ρ also evolves more rapidly, reflecting quicker population transfers. Its off-diagonal elements (coherences) decay faster if dephasing is present, hence all C_0 , C_{rel} , and C_{zz} diminish.

The order of $\tau_{C_{\text{rel}}}$ and τ_{C_0} lies in their operational definitions: C_{rel} is an entropy-based measure which detects the purely incoherent part of the density operator, while $C_0 = \langle \sigma_i^+ \sigma_j^- \rangle$ can only be non-zero if the density operator has off-diagonal elements. This relationship hence suggests that enhanced relative coherence drives corre-

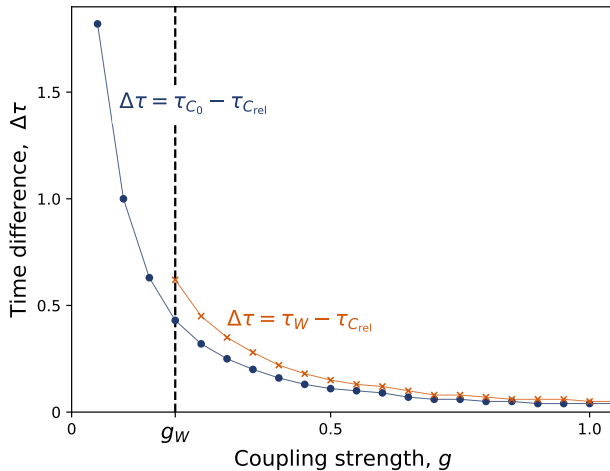


FIG. 5. (Color online) Time gaps, $\Delta\tau = \tau_{C_0} - \tau_{C_{\text{rel}}}$ and $\Delta\tau = \tau_W - \tau_{C_{\text{rel}}}$ are displayed for $N = 2$ as functions of g . The vertical dashed line ($g_W \approx 0.20$) represents the interaction strength above which entanglement is detected. Other parameters: $n_p = 1$, $\gamma = 0.1$, $\kappa = 0.1$, and $\gamma_\phi = 0.0225$.

lated emission. Moreover, $\langle W \rangle$ is also related to C_0 and to correlated dephasing, C_{zz} . Hence, if $C_{zz} \approx 0$, the entanglement is in one-to-one correspondence to C_0 and their time gap vanishes.

Conclusion — We investigated the time evolution of superradiance, coherence, and entanglement, and the interplay of their associated time scales, showing that these quantities have a clear temporal order: coherence builds up first, followed by the correlated emission peak, and then entanglement reaches its strongest form. At the very last, correlated dephasing reaches its minimum. We could show that enhanced relative coherence drives correlated emission. In summary:

$$\tau_{C_{\text{rel}}} \leq \tau_{C_0} \leq \tau_W \leq \tau_{C_{zz}}.$$

In light of a number of recent investigations of the sub- and superradiance decay dynamics [21–25], some of which are demonstrating that the current experimental capability is already sufficient to test our prediction, we expect that our results can be readily and directly verified in small systems in the near future.

Acknowledgements Support from the University of Otago, the Dodd-Walls Centre and Quantum Technologies Aotearoa is appreciatively recognized by N. F. Binti Rahimi. C. Gies gratefully acknowledges financial support from the German Federal Ministry of Research, Technology and Space (BMFTR) during his research sabbatical at the University of Otago.

- [1] R. H. Dicke, Physical Review **93**, 99 (1954).
- [2] K. Hepp and E. H. Lieb, Annals of Physics **76**, 360 (1973).
- [3] W.-K. Mok, A. Asenjo-Garcia, T. C. Sum, and L.-C. Kwek, Physical Review Letters **130**, 213605 (2023).
- [4] Superradiance and superfluorescence are similar phenomena, but in the former case a macroscopic dipole moment is created at the initialization, while in the latter case – due to incoherent initialization – no such dipole moment is present at the end of the initialization. Hence in superradiance there is an experimentally controlled direction (i.e., given by the dipole moment), which also influences the observed effect: superfluorescence aligns to random dipoles while superradiance aligns to the initially induced dipole.
- [5] V. Paulisch, M. Perarnau-Llobet, A. González-Tudela, and J. I. Cirac, Phys. Rev. A **99**, 043807 (2019).
- [6] S. L. Kristensen, E. Bohr, J. Robinson-Tait, T. Zelevinsky, J. W. Thomsen, and J. H. Müller, Phys. Rev. Lett. **130**, 223402 (2023).
- [7] D. Barberena, R. J. Lewis-Swan, A. M. Rey, and J. K. Thompson, Comptes Rendus. Physique **24**, 55 (2023).
- [8] M. A. Norcia, M. N. Winchester, J. R. K. Cline, and J. K. Thompson, Science Advances **2**, e1601231 (2016).
- [9] M. A. Norcia, J. R. K. Cline, J. A. Muniz, J. M. Robinson, R. B. Hutson, A. Goban, G. E. Marti, J. Ye, and J. K. Thompson, Phys. Rev. X **8**, 021036 (2018).
- [10] T. Laske, H. Winter, and A. Hemmerich, Phys. Rev. Lett. **123**, 103601 (2019).
- [11] M. Asada, Journal of Applied Physics **94**, 677 (2003), https://pubs.aip.org/aip/jap/article-pdf/94/1/677/19274909/677_1.online.pdf.
- [12] T. V. Teperik and A. Degiron, Phys. Rev. Lett. **108**, 147401 (2012).
- [13] D.-W. Wang and M. O. Scully, Phys. Rev. Lett. **113**, 083601 (2014).
- [14] N. Skribanowitz, I. P. Herman, J. C. MacGillivray, and M. S. Feld, Phys. Rev. Lett. **30**, 309 (1973).
- [15] M. Gross, C. Fabre, P. Pillet, and S. Haroche, Phys. Rev. Lett. **36**, 1035 (1976).
- [16] C. Bradac, M. T. Johnsson, M. v. Breugel, B. Q. Baragiola, R. Martin, M. L. Juan, G. K. Brennen, and T. Volz, Nature Communications **8** (2017), 10.1038/s41467-017-01397-4.
- [17] G. Rainò, M. A. Becker, M. I. Bodnarchuk, R. F. Mahrt, M. V. Kovalenko, and T. Stöferle, Nature **563**, 671–675 (2018).
- [18] T. P. T. Nguyen, L. Z. Tan, and D. Baranov, The Journal of Chemical Physics **159**, 204703 (2023).
- [19] K. Huang, K. K. Green, L. Huang, H. Hallen, G. Han, and S. F. Lim, Nature Photonics **16**, 737–742 (2022).
- [20] F. Jahnke, C. Gies, M. Aßmann, M. Bayer, H. A. M. Leymann, A. Foerster, J. Wiersig, C. Schneider, M. Kamp, and S. Höfling, Nature Communications **7** (2016), 10.1038/ncomms11540.
- [21] F. Lohof, D. Schumayer, D. A. W. Hutchinson, and C. Gies, Physical Review Letters **131**, 063601 (2023).
- [22] N. S. Bassler, “Absence of Entanglement Growth in Dicke Superradiance,” (2025), arXiv:2504.13646 [quant-ph].
- [23] P. Rosario, L. O. R. Solak, A. Cidrim, R. Bachelard, and J. Schachenmayer, Phys. Rev. Lett. **135**, 133602 (2025).
- [24] G. Ferioli, I. Ferrier-Barbut, and A. Browaeys, Phys. Rev. Lett. **134**, 153602 (2025).
- [25] X. H. H. Zhang, D. Malz, and P. Rabl, Phys. Rev. Lett. **135**, 033602 (2025).

- [26] N. Lambert, C. Emery, and T. Brandes, Phys. Rev. Lett. **92**, 073602 (2004).
- [27] V. M. Bastidas, C. Emery, B. Regler, and T. Brandes, Phys. Rev. Lett. **108**, 043003 (2012).
- [28] P. Kirton, M. M. Roses, J. Keeling, and E. G. Dalla Torre, Advanced Quantum Technologies **2**, 1800043 (2019).
- [29] M. M. Roses and E. G. Dalla Torre, PLOS ONE **15**, e0235197 (2020).
- [30] P. Das, S. Wüster, and A. Sharma, Physical Review A **109**, 013715 (2024).
- [31] B. M. Garraway, Philosophical Transactions of the Royal Society A: Mathematical, Physical and Engineering Sciences **369**, 1137 (2011).
- [32] E. Lu, B. Shanker, and C. Piermarocchi, Phys. Rev. A **107**, 043703 (2023).
- [33] J.-H. Lü, P.-R. Han, W. Ning, X. Zhu, F. Wu, L.-T. Shen, Z.-B. Yang, and S.-B. Zheng, Opt. Express **31**, 41669 (2023).
- [34] C. Liu, A. Di Falco, and A. Fratalocchi, Phys. Rev. X **4**, 021048 (2014).
- [35] N. Shammah, S. Ahmed, N. Lambert, S. De Liberato, and F. Nori, Physical Review A **98**, 063815 (2018).
- [36] J. R. Johansson, P. D. Nation, and F. Nori, Computer Physics Communications **183**, 1760 (2012).
- [37] J. R. Johansson, P. D. Nation, and F. Nori, Computer Physics Communications **184**, 1234 (2013).
- [38] T. Baumgratz, M. Cramer, and M. B. Plenio, Physical Review Letters **113**, 140401 (2014).
- [39] P. Krammer, H. Kampermann, D. Bruß, R. A. Bertlmann, L. C. Kwek, and C. Macchiavello, Phys. Rev. Lett. **103**, 100502 (2009).
- [40] A. V. Andreev, V. I. Emel'yanov, and Y. A. Il'inskiĭ, Soviet Physics Uspekhi **23**, 493 (1980).
- [41] N. E. Nefedkin, E. S. Andrianov, A. A. Zyablovsky, A. A. Pukhov, A. P. Vinogradov, and A. A. Lisyansky, Optics Express **25**, 2790 (2017).
- [42] M. Koppenhöfer, P. Groszkowski, H.-K. Lau, and A. Clerk, PRX Quantum **3**, 030330 (2022).
- [43] J. T. Young, E. Chaparro, A. P. Orioli, J. K. Thompson, and A. M. Rey, “Engineering One Axis Twisting via a Dissipative Berry Phase Using Strong Symmetries,” (2024).
- [44] A. Streltsov, U. Singh, H. S. Dhar, M. N. Bera, and G. Adesso, Phys. Rev. Lett. **115**, 020403 (2015).